Received: 11 January 2021 | Revised: 15 April 2021 | Accepted: 30 May 2021

DOI: 10.1002/bit.27846

ARTICLE

BIOTECHNOLOGY AND BIOENGINEERING WILEY

Model-based control for column-based continuous viral inactivation of biopharmaceuticals

Moo Sun Hong[1] | Amos E. Lu[1] | Rui Wen Ou[2] | Jacqueline M. Wolfrum[3] | Stacy L. Springs[3] | Anthony J. Sinskey[2] | Richard D. Braatz[1]

[1]Department of Chemical Engineering, Massachusetts Institute of Technology, Cambridge, Massachusetts, USA

[2]Department of Biology, Massachusetts Institute of Technology, Cambridge, Massachusetts, USA

[3]Center for Biomedical Innovation, Massachusetts Institute of Technology, Cambridge, Massachusetts, USA

Correspondence
Richard D. Braatz, Department of Chemical Engineering, Massachusetts Institute of Technology, 77 Massachusetts Ave, Cambridge, MA, USA.
Email: braatz@mit.edu

Funding information
U.S. Food and Drug Administration, Grant/Award Number: U01FD006483

Abstract

Batch low-pH hold is a common processing step to inactivate enveloped viruses for biologics derived from mammalian sources. Increased interest in the transition of biopharmaceutical manufacturing from batch to continuous operation resulted in numerous attempts to adapt batch low-pH hold to continuous processing. However, control challenges with operating this system have not been directly addressed. This article describes a low-cost, column-based continuous viral inactivation system constructed with off-the-shelf components. Model-based, reaction-invariant pH controller is implemented to account for the nonlinearities with Bayesian estimation addressing variations in the operation. The residence time distribution is modeled as a plug flow reactor with axial dispersion in series with a continuously stirred tank reactor, and is periodically estimated during operation through inverse tracer experiments. The estimated residence time distribution quantifies the minimum residence time, which is used to adjust feed flow rates. Controller validation experiments demonstrate that pH and minimum residence time setpoint tracking and disturbance rejection are achieved with fast and accurate response and no instability. Viral inactivation testing demonstrates tight control of logarithmic reduction values over extended operation. This study provides tools for the design and operation of continuous viral inactivation systems in service of increasing productivity, improving product quality, and enhancing patient safety.

KEYWORDS
bioprocess engineering, continuous processing, viral inactivation

1 | INTRODUCTION

The continuous manufacturing of biologics has been of interest to both academia and industry due to reduced costs, increased flexibility, ease of standardization and scale up, and improvements in product quality (Hong et al., 2018, 2020; Konstantinov & Cooney, 2015). In continuous manufacturing, viral removal has received much less attention than other unit operations such as bioreactors and chromatography. Biologics derived from mammalian sources are expected to undergo two orthogonal virus removal processes to remove/inactivate adventitious viruses or retrovirus-like particles that may be present in the master cell bank (ICH, 1999; Miesegaes et al., 2010; WHO, 2004). One common processing step is a batch low-pH hold to inactivate enveloped viruses (Shukla et al., 2007).

Moo Sun Hong and Amos E. Lu contributed equally to this study.

Methods for adapting low-pH hold to continuous processing have involved cyclic batch operation (Pall Life Sciences, 2018), continuous-flow tubular reactors (Amarikwa et al., 2019; Coolbaugh et al., 2021; Gillespie et al., 2019; Klutz et al., 2016; Orozco et al., 2017; Parker et al., 2018), and continuous-flow column-based reactors (Arnold et al., 2019; Martins et al., 2019, 2020; Senčar et al., 2020). None of the continuous-flow reactors, however, directly address control considerations with operating the systems. The operating pH and the residence time distribution (RTD) are critical process parameters (CPPs) in determining viral clearance and can impact product quality from over-incubation or excessive pH adjustment.

This article describes a low-cost, column-based continuous viral inactivation system constructed with off-the-shelf components. A fast and accurate model-based pH feedback control scheme allows for rapid startup and effective disturbance rejection. The RTD is estimated periodically during operation through injecting UV-transparent "*inverse*" tracer and used to estimate minimum residence time (MRT), which in turn is used to adjust feed flow rates. Controller validation experiments demonstrated its performance in pH and MRT setpoint tracking and feed buffer and column residence time disturbance rejection. Viral inactivation testing demonstrated tight control of logarithmic reduction values (LRVs) over extended operation.

2 | MATERIALS AND METHODS

2.1 | Viral inactivation prototype

A laboratory-scale continuous viral inactivation system was constructed (Figure 1). A multi-channel peristaltic pump (Ismatech Reglo ICC, 12 roller, 4 channel, 0.51/0.19 mm ID Pharmed BPT tubing) was used to pump input solution and acid to a mixing unit comprised of an in-line mixer (Stamixco, Model HT) and a peristaltic pump

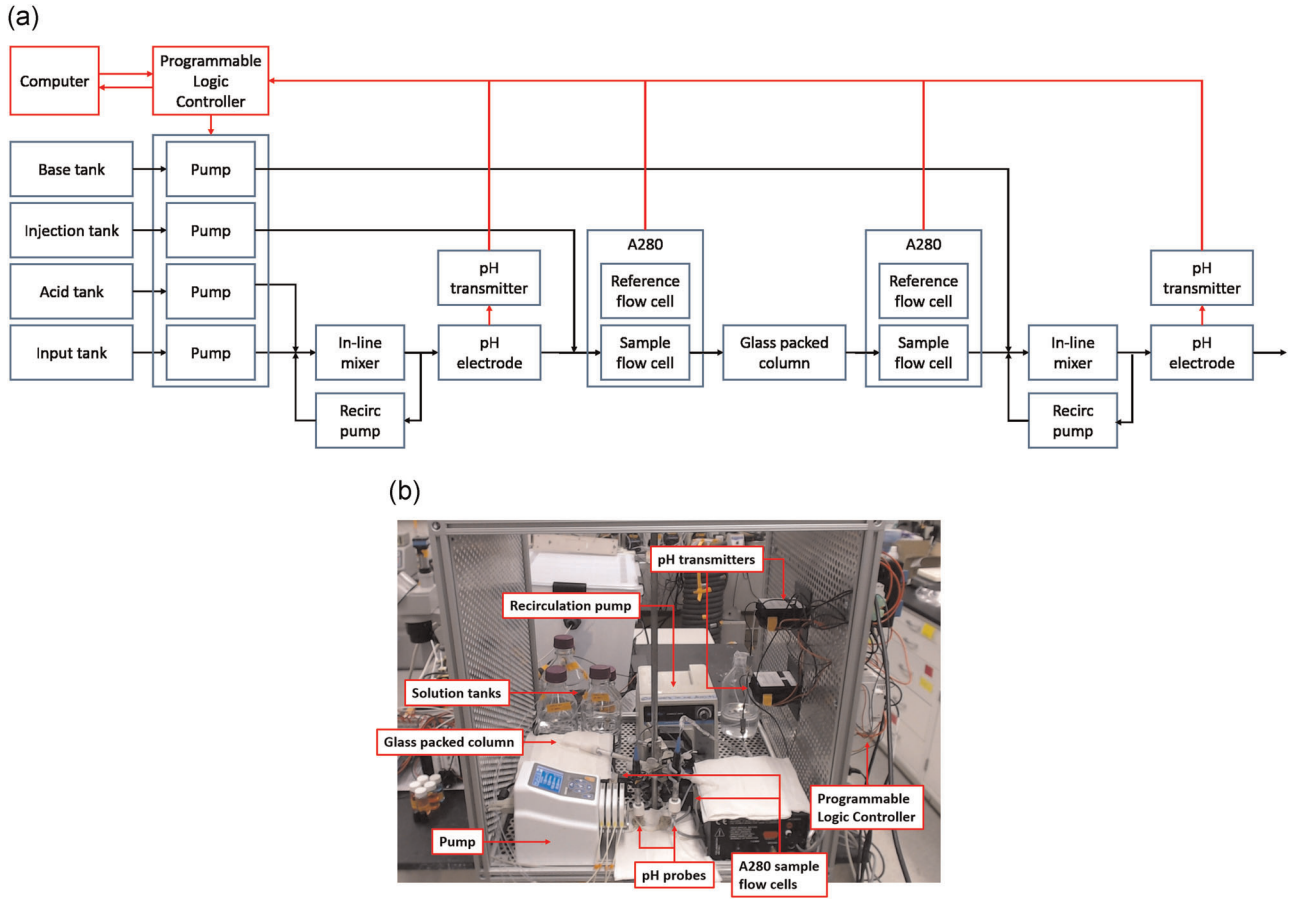

FIGURE 1 (a) Schematic of the column-based viral inactivation unit. The black lines indicate fluid flow, and the red lines indicate information flow. Input solution containing biologics is mixed with acid to lower the pH. This fluid is then directed to an inert glass-packed column for incubation at a specified residence time to inactivate viruses. This fluid is then mixed with base in a second mixing unit. pH electrodes are installed after each mixing unit to provide feedback to control acid and base flows. A protein-free injection solution is periodically added before the column. The fluid pulse is monitored before and after the column using UV absorbance at 280 nm, and used to characterize the residence time distribution of the column in real time. The total fluid flow to the system is adjusted to maintain the minimum residence time for viral inactivation assurance. (b) Photo of the column-based viral inactivation unit. Key components in the prototype are labeled. All components are commercial off-the-shelf equipment. UV, ultraviolet [Color figure can be viewed at wileyonlinelibrary.com]

(Masterflex L/S 14, Tygon E-Lab tubing). The mixed stream flows into an in-line pH electrode (Cole Parmer, Sealed, 800 μl volume), and into a column (Diba Omnifit EZ, 6.6 mm diameter, 250 mm length) packed with inert glass (Sigma-Aldrich; glass beads, 75 μm). An injection system is used to periodically inject UV-transparent solution into the flow stream, with UV absorbance sensors (Spectrum Labs, UV Model 280) at both the column inlet and outlet to measure column transit. The pH of the fluid leaving the column is raised by mixing with base using a second mixing unit and pH electrode.

A programmable logic controller (PLC, Koyo Click C0-11DD1E-D) was used for low-level control of the system. The multi-channel peristaltic pump was connected and actuated using the RS-232 interface. The pH transmitter (Cole Parmer, Model 350) was connected using 4–20 mA current loop (Koyo Click C0-04AD-1), while the absorbance sensor was connected using an analog voltage sensor (Koyo Click C0-04AD-2). The PLC was connected via MODBUS TCP to a touch-screen tablet (Microsoft Surface Go MCZ-00001) for data collection, human-machine interface, and online parameter estimation. In the PLC, a low-pass filter was applied to smooth the pH readings.

A model-based, reaction-invariant controller with Bayesian estimation was used for pH control (Lu et al., 2016). Bayesian estimation was performed on the tablet (using custom code running in MATLAB 2019a), and the parameter estimates forwarded to the PLC to improve the performance and robustness of the reaction-invariant controller. Real-time RTD parameter estimation and MRT estimation were also performed on the attached tablet for RTD monitoring and control, and the results forwarded to the PLC for closed-loop control of MRT.

2.2 | Controller validation

0.1 M sodium hydroxide with 1% (v/v) acetone was used as the test input solution. One molar phosphoric acid was used as the acid, and 1 M sodium hydroxide was used as the base. The low-absorbance injection solution was DIW. The acid was replaced with 0.5 M citric acid for the pH controller disturbance testing. A 30 cm loop of 1/16" ID tubing was added to the front of the column using two tees and pinch clamps was used to remove the loop from the flow path during operation for RTD controller disturbance testing.

2.3 | Viral inactivation validation

The test input solution was Phi6 storage buffer (15 mM phosphate, pH 7.3, 0.15 M KCl) with 50 mg/L tryptophan and $\sim 3 \times 10^7$ pfu/ml Phi6 bacteriophage. The Phi6 bacteriophage is widely used as a surrogate for enveloped viruses. This system has the advantages of (i) nonpathogenicity to humans, (ii) physiological similarity to mammalian enveloped viruses,[1] and (iii) easy cultivation, rapid analysis, and cost-effective assays (Aquino de Carvalho et al., 2017).

[1]Phi6 bacteriophage has an envelope.

Phi6 bacteriophage and host bacteria, *Pseudomonas syringae*, were kindly provided by Dr. Leonard Mindich (Public Health Research Institute). *P. syringae* bacteria were grown to exponential phase of an optical density at 600 nm (OD_{600}) of 0.1 to 0.2 in 1 L of modified LB medium (10 g/L tryptone, 5 g/L yeast extract, 5 g/L NaCl), and then infected with Phi6 bacteriophage at a multiplicity of infection (MOI) of 10 for 24 h at 25°C. After 24 h of growth, 20 U of bovine pancreatic DNase I (Roche) was added, followed by incubation at room temperature for 30 min, and NaCl was added to a final concentration of 0.5 M, followed by incubation on ice for 1 h. The cell and phage were then centrifuged at 11,000*g* for 10 min at 4°C. The phage in the cleared lysate was precipitated by addition of polyethylene glycol (Sigma-Aldrich, molecular weight 8000) to a final concentration of 11%. After the polyethylene glycol homogenized with the cell and phage culture, it was centrifuged at 11,000*g* for 10 min at 4°C. The precipitate was resuspended with 7.5 ml of SM buffer (5.8 g NaCl, 2 g $MgSO_4 \cdot 7H_2O$, 50 ml 1 M Tris–HCl, pH 7.5, and 5 ml 2% gelatin solution in 1 L water) with addition of CsCl to a final concentration of 0.75 g/ml for ultracentrifugation at 36,000 rpm (Beckman, SW-40 rotor) for 24 h at 4°C (modified from Kannoly et al., 2012). The band fractions were collected from the tube. The band fractions were used to identify the Phi6 titer by plaque spot assay. The phage samples were then dialyzed for 3 days with three changes of Phi6 storage buffer in 4°C cold room (Day & Mindich, 1980). The phage samples were passed through 0.2 μm PTFE membrane filters (VWR).

Phi6 phage titer was analyzed by phage plaque assay. Serial 1:10 dilution of samples were performed in Phi6 assay buffer (21 mM Na_2HPO_4, 11 mM KH_2PO_4, 43 mM NaCl, 9.3 mM NH_4Cl, 0.4 mM $MgSO_4$, pH 6.5). Ten microliters of diluted samples or 10 or 200 μl of samples were spotted on the solidified overlay of modified LB medium agar (10 g/L tryptone, 5 g/L yeast extract, 5 g/L NaCl, 7.5 g/L agar) containing overnight *P. syringae* (3 ml of modified LB medium and 1 ml of overnight *P. syringae* mixed with 3 ml of modified LB medium agar), then swirled slowly to spread the samples. The plates were dried at room temperature, and then incubated at 25°C for overnight. On the next day, the plaques were counted.

3 | RESULTS AND DISCUSSIONS

3.1 | Modeling and control of pH

In the inactivation process, fluid must first be brought to a low-pH state. Fast and accurate control of pH is necessary for rapid inactivation while minimizing impact to product quality. A model-based, reaction-invariant controller is used here to account for the nonlinearities present in a typical buffer titration curve. To maintain constant total flow rate through the column, the controller manipulates flow ratio instead of flow rate. The pH control system must also address changing product and buffer concentration due to

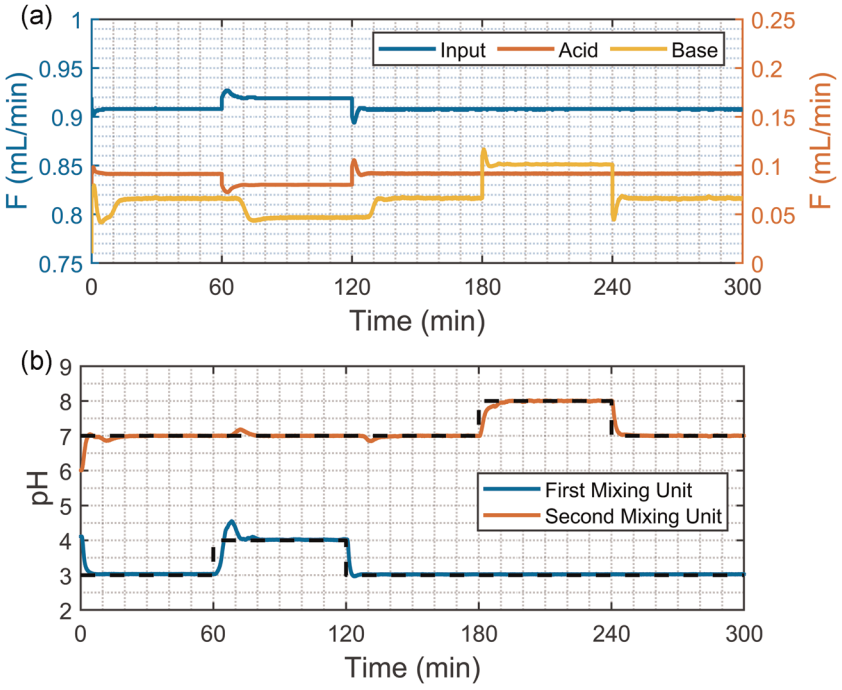

FIGURE 2 pH controller setpoint tracking. (a) Flow rates determined by the pH controller and (b) pH measurements. The black dashed lines indicate setpoints. The pH setpoint for the first mixing unit was changed from 3 to 4 at 60 min and back to 3 at 120 min. The pH setpoint for the second mixing unit was changed from 7 to 8 at 180 min and back to 7 at 240 min. Fast and accurate response was observed with no instability [Color figure can be viewed at wileyonlinelibrary.com]

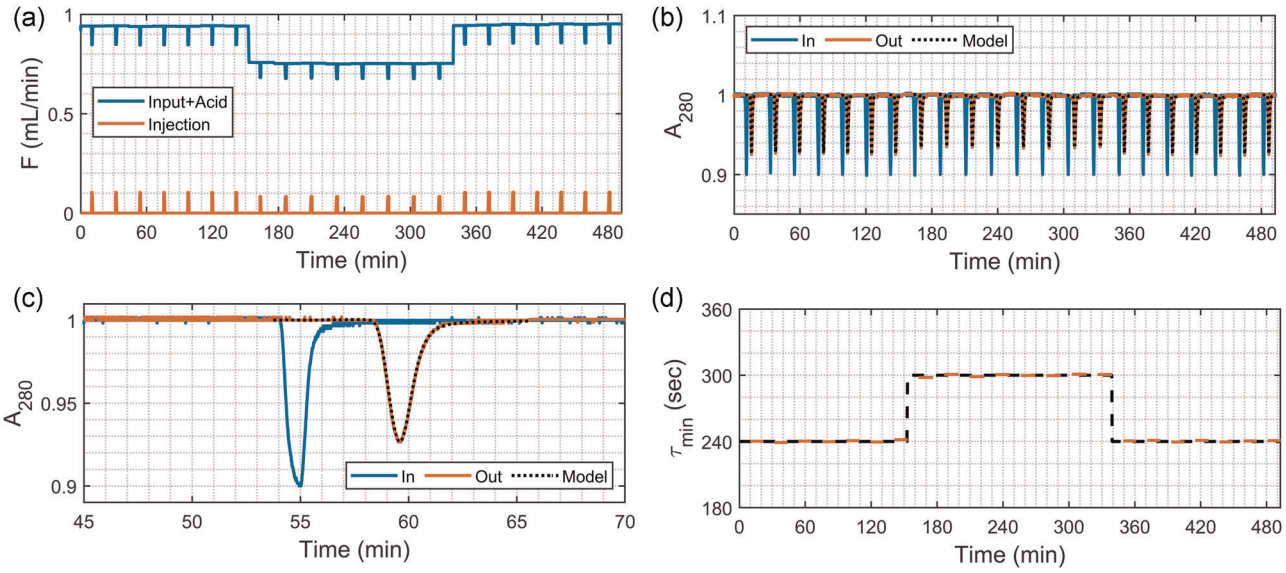

FIGURE 3 MRT controller setpoint tracking. (a) Flow rates determined by the MRT controller, (b,c) absorbance measurements at the inlet and outlet of the column, and (d) estimated MRT with setpoints. The black dashed lines indicate setpoints. The MRT setpoint was changed from 4 min to 5 min at 180 min and back to 4 min at 360 min. Setpoint tracking was achieved within a single step. The RTD model accurately predicts the concentration at the outlet. MRT, minimum residence time; RTD, residence time distribution [Color figure can be viewed at wileyonlinelibrary.com]

natural or unexpected variation in bioreactor or capture column operation. Bayesian estimation is used to address these uncertainties by updating solution pK_a and concentrations in response to sensor data. For implementation details on the pH modeling and controller design, the reader is referred to previously published work (Lu et al., 2016).

3.2 | Design of the column-based inactivation reactor

A packed-bed column-based system was chosen due to its narrow residence time distribution and that there is substantial industrial experience in packing and qualifying columns to ensure uniformity.

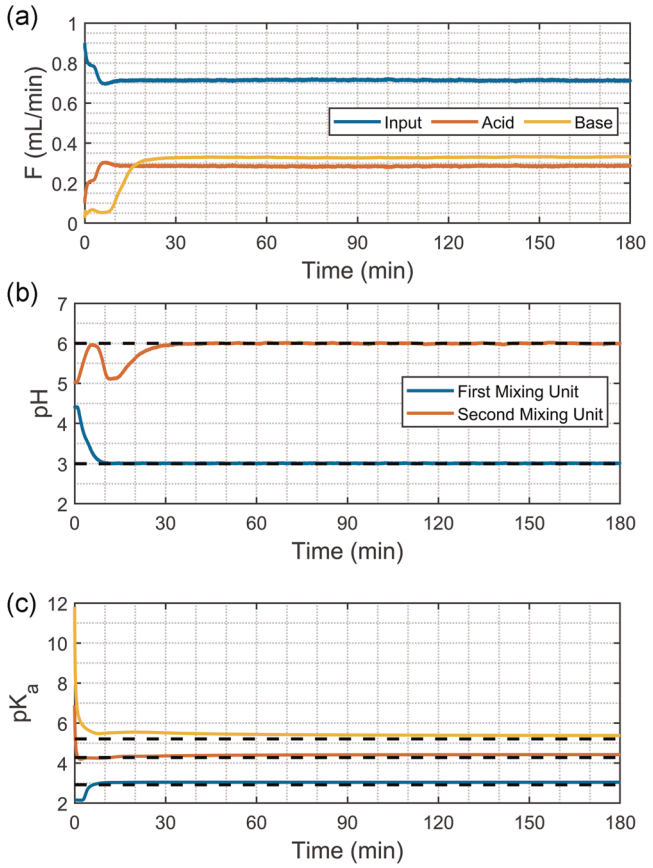

FIGURE 4 pH controller disturbance rejection. (a) Flow rates determined by the pH controller and (b) pH measurements. The black dashed lines indicate setpoints. (c) Estimated pK_a values. The black dashed lines indicate the true values for citric acid. The system was started with citric acid instead of phosphoric acid despite the model being initialized with the phosphoric acid parameters, to demonstrate the ability to control the system in the presence of large disturbances. The Bayesian estimation algorithm correctly estimates the new pK_a value. Fast and accurate response was observed with no instability [Color figure can be viewed at wileyonlinelibrary.com]

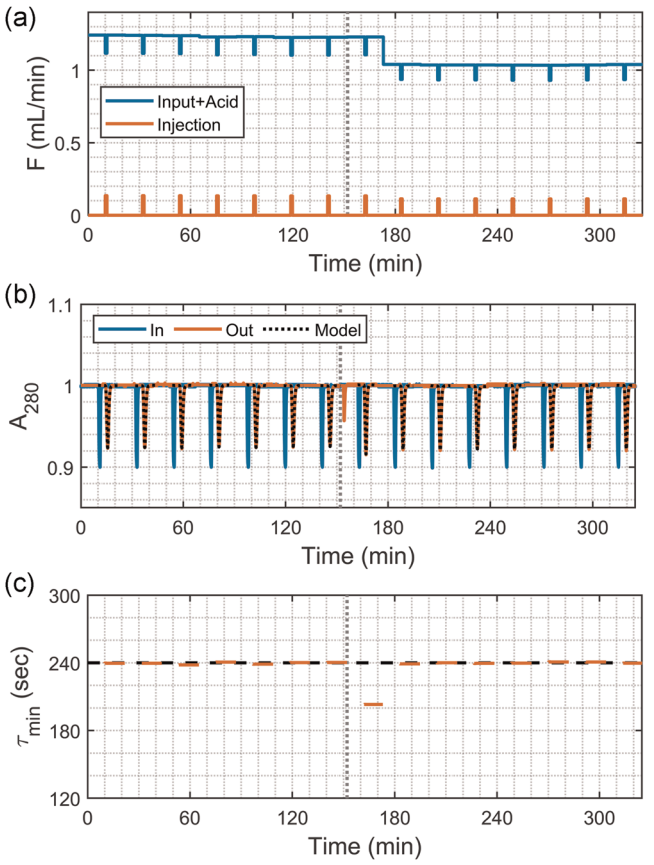

FIGURE 5 MRT controller disturbance rejection. (a) Flow rates determined by the MRT controller, (b) absorbance measurements at the inlet and outlet of the column, and (c) estimated MRT. The black dashed line indicates setpoints. The vertical dotted lines represent the time when the system volume was reduced. The system was first started with an additional dead volume in front of the column. At 150 min, the dead volume was bypassed, reducing the system volume. The MRT measurement system correctly identifies the change in residence time and adjusts pump speed, restoring the original residence time setpoint in a single step. The model correctly predicts the output of each water injection. MRT, minimum residence time [Color figure can be viewed at wileyonlinelibrary.com]

The system is constructed from commercial off-the-shelf components, with glass beads selected for their inert nature and low risk of leaching.

The column is designed to provide a desired throughput and residence time, while having low pressure drop and dispersion. The design parameters are the column diameter d and length L, the particle size d_p, and the superficial velocity v_s. The desired volumetric flow rate Q and average residence time τ are related to the design parameters by

$$Q = \frac{\pi d^2 v_s}{4}, \quad \tau = \frac{L}{u} = \frac{\epsilon L}{v_s}, \tag{1}$$

where u is the mean velocity and ϵ is the column porosity which is about 0.4 for real packings (Zhang et al., 2006). The column diameter and length are chosen based on the desired throughput and residence time by $d = \sqrt{\frac{4Q}{\pi v_s}}$ and $L = \frac{\tau v_s}{\epsilon}$. The latter equation can be used to simplify the Kozeny-Carman equation (Carman, 1956) for the pressure drop in the column to

$$\Delta P = \frac{180\mu L}{\phi_s^2 d_p^2}\frac{(1-\epsilon)^2}{\epsilon^3}v_s = \frac{180\mu\tau(1-\epsilon)^2}{\phi_s^2\epsilon^4}\left(\frac{v_s}{d_p}\right)^2, \tag{2}$$

where μ is the fluid viscosity and ϕ_s is the particle sphericity. The standard deviation of a dispersed peak can be characterized as

$$\sigma = \sqrt{2\frac{DL}{u^3}} = 2\sqrt{\tau\frac{d_p}{v_s}}, \tag{3}$$

where dispersion coefficient is given by $D = \frac{2ud_p}{\epsilon}$ (Levenspiel, 1999). The particle size and superficial velocity appear in the right-hand sides of Equations (2) and (3) only as a ratio, and changing that ratio to reduce the pressure drop increases the dispersion, and vice versa. We chose the ratio to minimize the

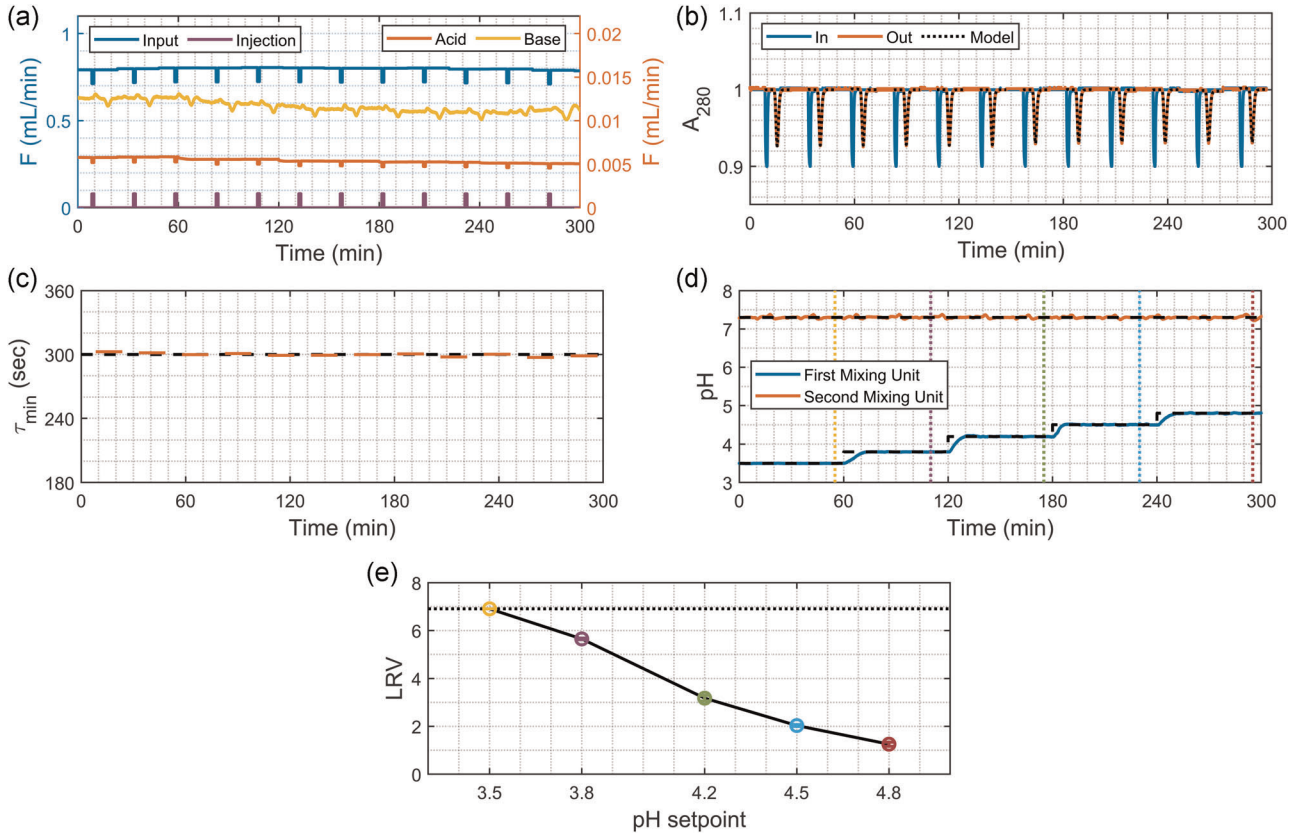

FIGURE 6 Viral inactivation with respect to pH. (a) Flow rates determined by the controllers, (b) absorbance measurements at the inlet and outlet of the column, (c) estimated MRT, and (d) pH measurements. The black dashed lines indicate setpoints. The vertical dotted lines represent the time when outlet from the system was sampled for the phage plaque assay. The pH setpoint for first mixing unit was changed from 3.5 to 3.8, 4.2, 4.5, and 4.8. The pH setpoint for second mixing unit was 7.3 and MRT setpoint was 5 min. (e) LRV values of the samples from varying pH setpoints for the first mixing unit. The horizontal dotted line shows the limit of detection (no live virus was detected for values on the horizontal dotted lines). LRV was decreased as pH setpoint for the first mixing unit was increased. LRV, logarithmic reduction value; MRT, minimum residence time [Color figure can be viewed at wileyonlinelibrary.com]

dispersion while satisfying the pressure limit of the peristaltic pump. To optimize compactness of the system, a small particle size and superficial velocity was chosen, among the commercially available columns and glass beads.

3.3 | Modeling of the RTD

The low pH solution must be incubated for a sufficient time for viral inactivation. At the same time, extended incubation can result in aggregation and the formation of acidic species, degrading product quality. A quantitative understanding of the process is necessary to balance between these two competing effects. This understanding comes from a RTD, which describes the amount of time that a fluid element spends within the system by a probability distribution function E.

The column can be modeled as a plug flow reactor (PFR) with axial dispersion in series with a continuously stirred tank reactor (CSTR), with the respective RTDs (Levenspiel, 1999)

$$E_{\mathrm{PFR}}(\theta, \mathrm{Pe}, x) = \sqrt{\frac{\mathrm{Pe}}{4\pi x\theta}} \exp\left(-\frac{\mathrm{Pe}(x-\theta)^2}{4x\theta}\right), \tag{4}$$

$$E_{\mathrm{CSTR}}(\theta, x) = \frac{1}{1-x} \exp\left(-\frac{\theta}{1-x}\right), \tag{5}$$

where Pe is the Peclet number, x is the residence time fraction of PFR, and $\theta(t, \tau)$ is the dimensionless time. The concentration of any component at the outlet of the column can be calculated through the convolution

$$C_{\mathrm{out}}(\theta) = C_{\mathrm{in}}(\theta) * E(\theta, \mathrm{Pe}, x) = \int_0^{\theta} C_{\mathrm{in}}(\theta - \theta') E(\theta', \mathrm{Pe}, x) \mathrm{d}\theta', \tag{6}$$

$$E(\theta, \mathrm{Pe}, x) = E_{\mathrm{PFR}}(\theta, \mathrm{Pe}, x) * E_{\mathrm{CSTR}}(\theta, x) = \int_0^{\theta} E_{\mathrm{PFR}}(\theta - \theta', \mathrm{Pe}, x) E_{\mathrm{CSTR}}(\theta', x) \mathrm{d}\theta'. \tag{7}$$

The cumulative distribution function F can be computed as

$$F(\theta, \mathrm{Pe}, x) = \int_0^{\theta} E(\theta', \mathrm{Pe}, x) \mathrm{d}\theta', \tag{8}$$

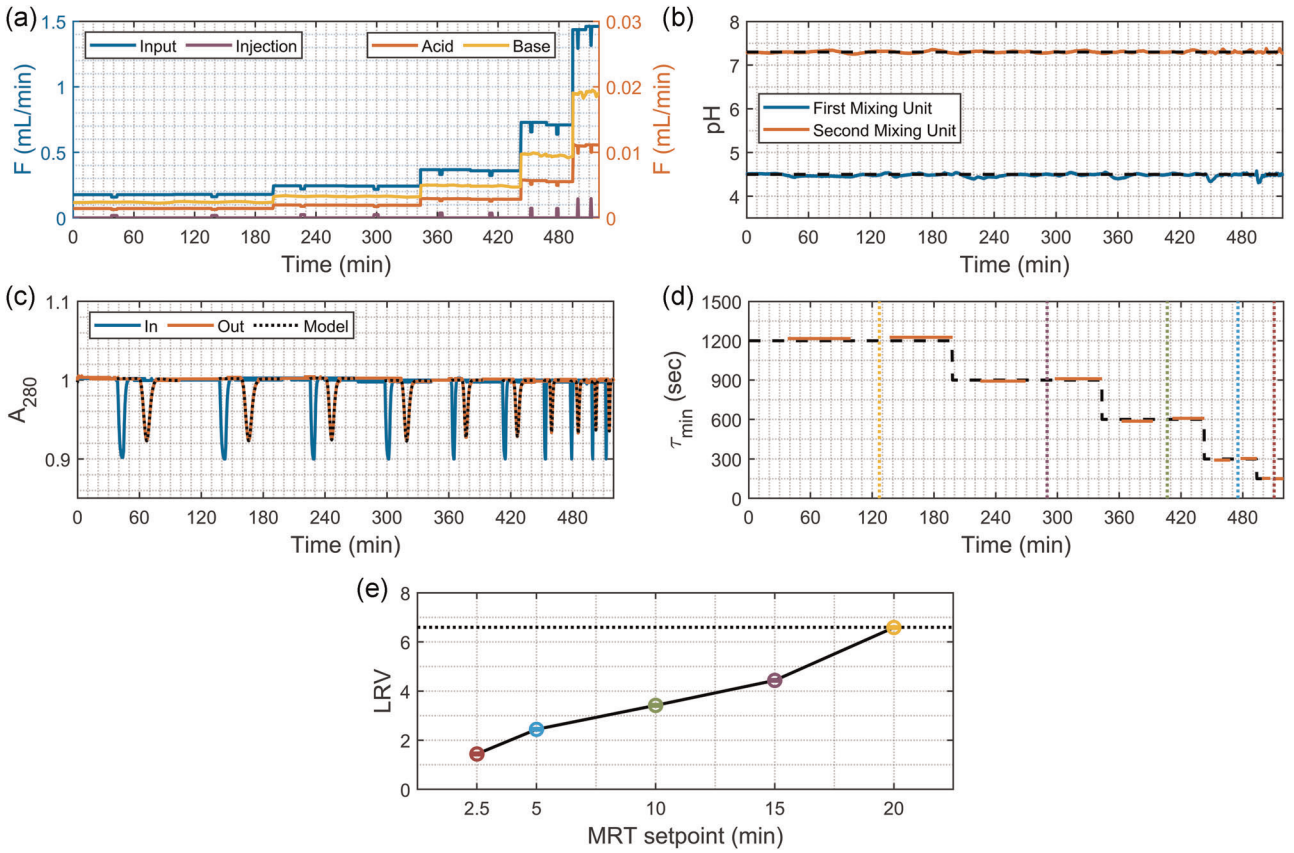

FIGURE 7 Viral inactivation with respect to the MRT. (a) Flow rates determined by the controllers, (b) pH measurements, (c) absorbance measurements at the inlet and outlet of the column, and (d) estimated MRT. The black dashed lines indicate setpoints. The vertical dotted lines represent the time when the outlet from the system was sampled for the phage plaque assay. The MRT setpoint was changed from 20 min to 15, 10, 5, and 2.5 min. The pH setpoint for the first mixing unit was 4.5 and the pH setpoint for the second mixing unit was 7.3. (e) LRV values of the samples for varying MRT setpoints. The horizontal dotted line shows the limit of detection (no live virus was detected for values on the horizontal dotted lines). The LRV was decreased as the MRT setpoint decreased. LRV, logarithmic reduction value; MRT, minimum residence time [Color figure can be viewed at wileyonlinelibrary.com]

which in turn allows us to define the minimum residence time $\tau_{\min}$ as

$$F(\theta(\tau_{\min}, \tau), \mathrm{Pe}, x) = \eta, \tag{9}$$

where η is a small value corresponding to the fraction of material leaving before the minimum residence time.

3.4 | Control of residence time

The RTD is affected by variables such as reactor design, geometry, fouling, pump drift, and input flow rates which can be classified into three types. Manipulated variables such as input flow rates can be specified by the controller online. Disturbance variables are variables such as fouling and pump drift that vary during operation while not being specifiable by the controller. Design variables such as reactor design and geometry can only be controlled offline.

While design variables have been explored quite extensively in past work in continuous viral inactivation (Amarikwa et al., 2019; Coolbaugh et al., 2021; Gillespie et al., 2019; Klutz et al., 2016; Orozco et al., 2017; Parker et al., 2018), disturbance rejection has not been discussed directly. Disturbance rejection is especially important to consider when operating continuously for an extended period of time.

The effect of disturbances on the RTD cannot be completely rejected, since the RTD is infinite dimensional and the manipulated variables such as flow rates are scalars. A feasible alternative is to reject the effect of disturbances on a scalarized measure of the RTD. For example, a control system could be designed to reject the effect of disturbances on the LRV computed from the RTD using a nonlinear model (Senčar et al., 2020). An alternative approach is to reject the effect of disturbances on the (MRT), which is the time before which only a small fraction of material leaves. Values of this fraction reported in the literature range from 10^{-5} (Amarikwa et al., 2019) to 0.005 (Klutz et al., 2016; Orozco et al., 2017; Parker et al., 2018). Alternatively, the MRT has been defined by subtracting five standard deviations of the RTD from the average residence time (Brown & Orozco, 2021). While the LRV approach allows for direct addressing of the critical quality attribute (CQA) of LRV, it relies on an accurate viral inactivation model, which may vary from virus to virus and has

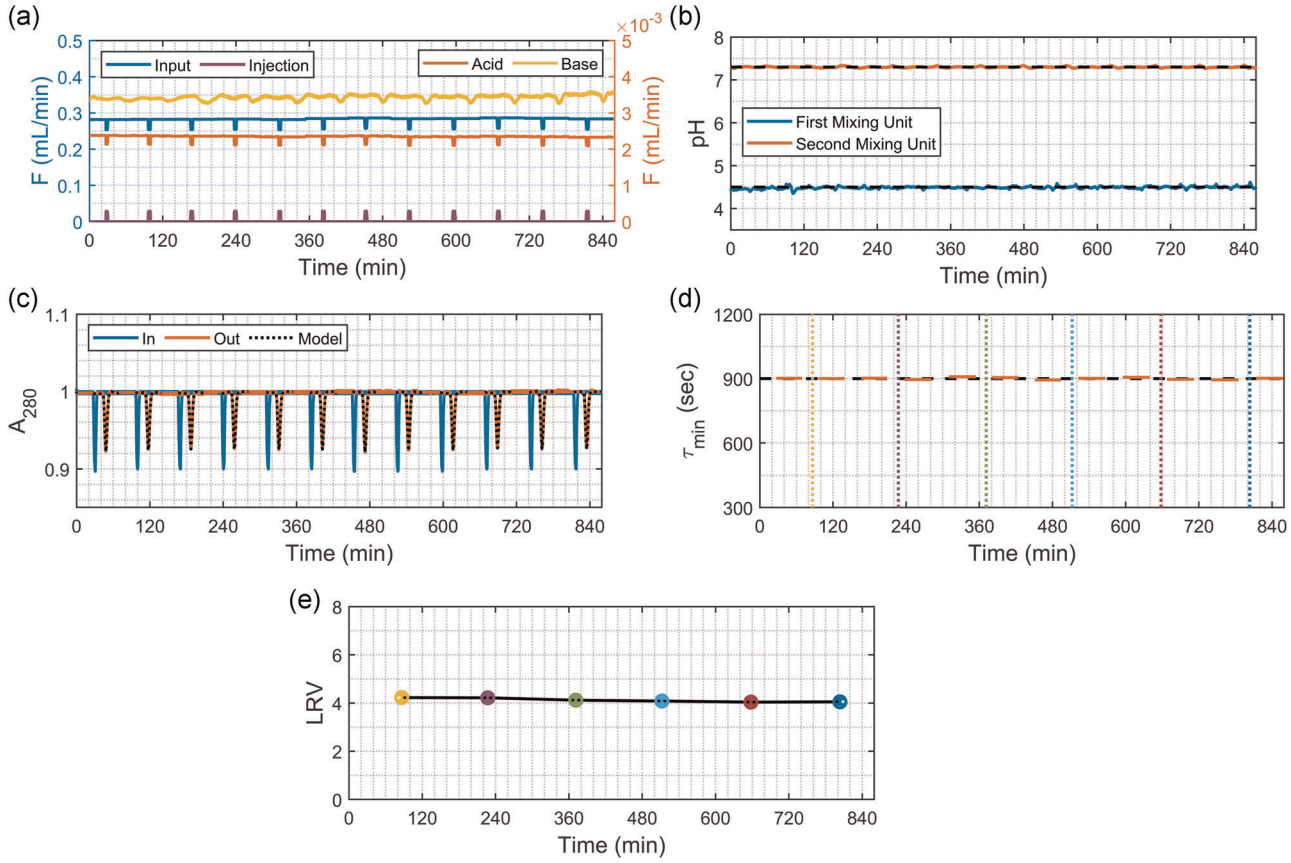

FIGURE 8 Viral inactivation while operating at a pH setpoint of 4.5 for the first mixing unit, a pH setpoint of 7.3 for the second mixing unit, and MRT setpoint of 15 min. (a) Flow rates determined by the controllers, (b) pH measurements, (c) absorbance measurements at the inlet and outlet of the column, and (d) estimated MRT. The black dashed lines indicate setpoints. The vertical dotted lines represent the time when the outlet from the system was sampled for the phage plaque assay. (e) LRV values of the samples from varying the operation time. The LRV was consistent over the operation period. LRV, logarithmic reduction value; MRT, minimum residence time [Color figure can be viewed at wileyonlinelibrary.com]

associated uncertainty. This uncertainty is avoided by utilizing the 0.005 fraction MRT approach.[2]

MRT control requires three components: (1) a means of measuring RTD/MRT, (2) a feedback control algorithm for adjusting flow rate in response to MRT, and (3) a means of actuating flow rate.

3.5 | Measurement of RTD and MRT

At the low values of η, direct measurement of MRT using tracer experiments is impossible due to in-line sensor noise obscuring observability. To overcome lack of observability, the RTD can be estimated as a parametric distribution, which can in turn be used to determine the MRT.

Using the Beer–Lambert law, the absorbance $A_{280}(t)$ is proportional to concentration $C(t)$ and can be written as

$$A_{280,\text{out}}(\theta) = A_{280,\text{in}}(\theta)^{*}E(\theta, \text{Pe}, x). \tag{10}$$

The parameters τ, Pe, and x can be calculated from the absorbance measurement through the solution of the sum-of-squares minimization

$$\underset{\tau,\text{Pe},x}{\text{argmax}} \int_0^T [A_{280,\text{in}}(\theta(t,\tau))^{*}E(\theta(t,\tau), \text{Pe}, x) - A_{280,\text{out}}(\theta(t,\tau))]^2 dt, \tag{11}$$

and used to estimate MRT through Equations (8) and (9).

The absorbance $A_{280,\text{in}}$ needs sufficient variability for accurate parameter estimation, which can be achieved through normal process variations, such as concentration peaks inherent in multi-column chromatography elution. In the case that the system is operated from a large, well-mixed tank and is devoid of variation, concentration variation would need to be deliberately introduced. This introduction is safely achieved through the periodic injection of deionized water (DIW), which has negligible UV absorbance relative to that of protein-laden input solution. This injection effectively dilutes the solution, lowering the absorbance, and providing the necessary variability.

[2]The controls in this article could be straightforwardly revised to use the 10^{-5} MRT approach, or the LRV approach if the viral inactivation kinetics are known.

3.6 | Feedback control algorithm and actuation

Given the MRT estimation, a feedback control algorithm

$$\omega_{i+1} = \frac{\omega_i \tau_{\min,i}}{\tau_{\min,SP}}, \quad (12)$$

where ω is the pump rotational speed and the subscripts i refers to the current time step, $i + 1$ refers to the next time step, and SP refers to the setpoint, can be used to provide a new pump speed.

Since peristaltic pump flow rates are nearly linear to rotational speed, the system can attain the setpoint within a single step after an RTD/MRT measurement. Any nonlinearity or disturbance (e.g., tubing stretch) is also addressed through feedback control. Using the feed flow rate for residence time control removes a degree of freedom in responding to changes in upstream flow into the unit. This can be solved by slightly diluting the product stream or introducing a surge tank.

3.7 | Controller validation experiments

The pH controllers had fast and accurate response with no instability while following step up and down of the pH setpoints (Figure 2). The MRT controller, for a step up and down of its setpoint, provided setpoint tracking within a single step after the RTD estimation (Figure 3). The RTD model with estimated parameters accurately predicted the concentration at the outlet with the concentration at the inlet (Figure 3c).

The ability of the control system to reject pH-related disturbances was demonstrated by changing the buffer of the acid stream fed to the system from phosphoric acid to citric acid. The system not only remained stable, but correctly estimated the pK_a of citric acid purely from the data obtained from the pH measurements in the first few minutes (Figure 4).

The ability of the control system to reject RTD-related disturbances was demonstrated by adding an additional length of tubing in series with the column. While the system is in normal operation, tube clamps were used to remove the additional length of tubing from the flow path, effectively subtracting dead volume and changing the system RTD. Despite this sudden change, the RTD was correctly measured and the MRT was correctly re-estimated (Figure 5). The controller adjusted the pump speeds immediately after receiving the new MRT and restored the MRT setpoint in a single step (Figure 5).

3.8 | Viral inactivation experiments

Viral inactivation was demonstrated by varying the pH setpoints from 3.5 to 4.8 at an MRT setpoint of 5 min (Figure 6). The Phi6 bacteriophage was below the limit of detection at pH 3.5 and inactivation kinetics were slower at the higher pH setpoints. Viral inactivation was also tested with varying MRT setpoints from 20 to 2.5 min at a pH setpoint of 4.5 (Figure 7). The Phi6 bacteriophage was below the limit of detection at a MRT of 20 min and the LRV values decreased at the lower MRT setpoints. Reproducibility of viral inactivation was tested at fixed setpoints of pH 4.5 and MRT 15 min for about 15 h (Figure 8). The system resulted in stable control of both pH and MRT during the operation. Collected samples during the operation also showed a consistent LRV value with a standard deviation of 0.08, which is smaller than standard deviations of triplicate analysis of each sample 0.12.

4 | CONCLUSION

This article describes a low-cost column-based continuous-flow viral inactivation system constructed with off-the-shelf components that provides tight control of the operating pH and minimum residence time (MRT). The system injects acid solution into the feed stream using a mixing unit whose outlet flows to an in-line pH electrode. pH measurements are used to adjust the flow rates to control the pH based on a model-based reaction-invariant controller that uses Bayesian estimation to ensure robustness. The mixed stream then flows into a column that has UV absorbance sensors at the inlet and outlet. UV-transparent inverse tracer is periodically injected into the flow stream to estimate the residence time distribution (RTD) and MRT, which is used to adjust feed flow rates to control the MRT based on a feedback control algorithm. The pH of the fluid leaving the column is raised by mixing with base solution whose flow rate is specified by the model-based controller.

Controller validation experiments for step changes in the setpoints and sudden disturbances demonstrate tight control of the pH and MRT. Bayesian estimation for pH control correctly estimates the pK_a values from the pH measurements and the RTD is correctly estimated from the absorbance measurements, which enable stable control of both the pH and MRT even with sudden disturbances. Viral inactivation experiments demonstrate the connection between the CPPs of operating pH and MRT and the CQA of LRV and tight control of both over extended operation.

The capability of the system to tightly control CPPs enables continuous operation of viral inactivation at optimal conditions not only for viral inactivation but also for product quality by preventing overincubation or excessive pH adjustment. Such a capability can contribute to increasing productivity, improving product quality, and enhancing patient safety of the continuous manufacturing of biologics.

ACKNOWLEDGMENTS

The authors thank Dr. Leonard Mindich for providing Phi6 bacteriophage and host bacteria, *Pseudomonas syringae*. This study is supported by the U.S. Food and Drug Administration, Grant No. U01FD006483. Any opinions, findings, conclusions, or recommendations expressed in this material are those of the authors and do not necessarily reflect the views of the financial sponsor. A provisional patent application has been submitted based on this study.

AUTHOR CONTRIBUTIONS

Conceptualization: Moo Sun Hong, Amos E. Lu, Richard D. Braatz; *system construction*: Moo Sun Hong, Amos E. Lu; *system modeling*:

Moo Sun Hong, Amos E. Lu; *system validation*: Moo Sun Hong; *phage plaque assay*: Rui Wen Ou; *writing —original draft*: Moo Sun Hong, Amos E. Lu, Rui Wen Ou; *writing—review and editing*: Moo Sun Hong, Amos E. Lu, Richard D. Braatz; *funding acquisition*: Richard D. Braatz, Anthony J. Sinskey, Stacy L. Springs, Jacqueline M. Wolfrum.

ORCID

Moo Sun Hong https://orcid.org/0000-0003-2274-5030
Stacy L. Springs https://orcid.org/0000-0003-2133-5689
Anthony J. Sinskey https://orcid.org/0000-0002-1015-1270
Richard D. Braatz https://orcid.org/0000-0003-4304-3484

REFERENCES

Amarikwa, L., Orozco, R., Brown, M., & Coffman, J. (2019). Impact of Dean vortices on the integrity testing of a continuous viral inactivation reactor. *Biotechnology Journal*, *14*(2), 1700726. https://doi.org/10.1002/biot.201800278

Aquino de Carvalho, N., Stachler, E. N., Cimabue, N., & Bibby, K. (2017). Evaluation of Phi6 persistence and suitability as an enveloped virus surrogate. *Environmental Science & Technology*, *51*(15), 8692–8700. https://doi.org/10.1021/acs.est.7b01296

Arnold, L., Lee, K., Rucker-Pezzini, J., & Lee, J. H. (2019). Implementation of fully integrated continuous antibody processing: Effects on productivity and COGm. *Biotechnology Journal*, *14*(2), 1800061. https://doi.org/10.1002/biot.201800061

Brown, M., & Orozco, R. (2021). Utilizing bacteriophage to define the minimum residence time within a plug flow reactor. *Biotechnology & Bioengineering*. https://doi.org/10.1002/bit.27734

Carman, P. C. (1956). *Flow of gases through porous media*. London: Butterworths Scientific Publications.

Coolbaugh, M. J., Varner, C. T., Vetter, T. A., Davenport, E. K., Bouchard, B., Fiadeiro, M., Tugcu, N., Walther, J., Patil, R., & Brower, K. (2021). Pilot-scale demonstration of an end-to-end integrated and continuous biomanufacturing process. *Biotechnology & Bioengineering*. https://doi.org/10.1002/bit.27670

Day, L. A., & Mindich, L. (1980). The molecular weight of bacteriophage θ 6 and its nucleocapsid. *Virology*, *103*(2), 376–385. https://doi.org/10.1016/0042-6822(80)90196-8

Gillespie, C., Holstein, M., Mullin, L., Cotoni, K., Tuccelli, R., Caulmare, J., & Greenhalgh, P. (2019). Continuous in-line virus inactivation for next generation bioprocessing. *Biotechnology Journal*, *14*(2), 1700718. https://doi.org/10.1002/biot.201800278

Hong, M. S., Severson, K. A., Jiang, M., Lu, A. E., Love, J. C., & Braatz, R. D. (2018). Challenges and opportunities in biopharmaceutical manufacturing control. *Computers & Chemical Engineering*, *110*, 106–114. https://doi.org/10.1016/j.compchemeng.2017.12.007

Hong, M. S., Sun, W., Lu, A. E., & Braatz, R. D. (2020). Process analytical technology and digital biomanufacturing of monoclonal antibodies. *American Pharmaceutical Review*, *23*(6), 122–125.

ICH. (1999). Viral safety evaluation of biotechnology products derived from cell lines of human or animal origin Q5A(R1). *ICH Harmonised Tripartite Guideline*.

Kannoly, S., Shao, Y., & Wang, I. N. (2012). Rethinking the evolution of single-stranded RNA (ssRNA) bacteriophages based on genomic sequences and characterizations of two R-plasmid-dependent ssRNA phages, C-1 and Hgal1. *Journal of Bacteriology*, *194*(18), 5073–5079. https://doi.org/10.1128/JB.00929-12

Klutz, S., Lobedann, M., Bramsiepe, C., & Schembecker, G. (2016). Continuous viral inactivation at low pH value in antibody manufacturing. *Chemical Engineering and Processing: Process Intensification*, *102*, 88–101. https://doi.org/10.1016/j.cep.2016.01.002

Konstantinov, K. B., & Cooney, C. L. (2015). White paper on continuous bioprocessing May 20-21, 2014 continuous manufacturing symposium. *Journal of Pharmaceutical Sciences*, *104*(3), 813–820. https://doi.org/10.1002/jps.24268

Levenspiel, O. (1999). *Chemical reaction engineering* (3rd ed.). Wiley.

Lu, A. E., Paulson, J. A., & Braatz, R. D. (2016). pH and conductivity control in an integrated biomanufacturing plant. In *Proceedings of the American Control Conference*, 1741–1746. https://doi.org/10.1109/ACC.2016.7525168

Martins, D. L., Sencar, J., Hammerschmidt, N., Flicker, A., Kindermann, J., Kreil, T. R., & Jungbauer, A. (2020). Truly continuous low pH viral inactivation for biopharmaceutical process integration. *Biotechnology & Bioengineering*, *117*(5), 1406–1417. https://doi.org/10.1002/bit.27292

Martins, D. L., Sencar, J., Hammerschmidt, N., Tille, B., Kinderman, J., Kreil, T. R., & Jungbauer, A. (2019). Continuous solvent/detergent virus inactivation using a packed-bed reactor. *Biotechnology Journal*, *14*(8), 1800646. https://doi.org/10.1002/biot.201800646

Miesegaes, G., Lute, S., & Brorson, K. (2010). Analysis of viral clearance unit operations for monoclonal antibodies. *Biotechnology & Bioengineering*, *106*(2), 238–246. https://doi.org/10.1002/bit.22662

Orozco, R., Godfrey, S., Coffman, J., Amarikwa, L., Parker, S., Hernandez, L., Wachuku, C., Mai, B., Song, B., Hoskatti, S., Asong, J., & Fiadeiro, M. (2017). Design, construction, and optimization of a novel, modular, and scalable incubation chamber for continuous viral inactivation. *Biotechnology Progress*, *33*(4), 954–965. https://doi.org/10.1002/btpr.2442

Pall Life Sciences. (2018). *Cadence virus inactivation system: automated semi-continuous low ph virus-inactivation on a single-use mixing platform* (Technical Report). Port Washington, NY. (Application Note USD3268)

Parker, S. A., Amarikwa, L., Vehar, K., Orozco, R., Godfrey, S., Coffman, J., Shamlou, P., & Bardliving, C. L. (2018). Design of a novel continuous flow reactor for low pH viral inactivation. *Biotechnology & Bioengineering*, *115*(3), 606–616. https://doi.org/10.1002/bit.26497

Senčar, J., Hammerschmidt, N., Martins, D. L., & Jungbauer, A. (2020). A narrow residence time incubation reactor for continuous virus inactivation based on packed beds. *New Biotechnology*, *55*, 98–107. https://doi.org/10.1016/j.nbt.2019.10.006

Shukla, A. A., Hubbard, B., Tressel, T., Guhan, S., & Low, D. (2007). Downstream processing of monoclonal antibodies—Application of platform approaches. *Journal of Chromatography B*, *848*(1), 28–39. https://doi.org/10.1016/j.jchromb.2006.09.026

WHO. (2004). Guidelines on viral inactivation and removal procedures intended to assure the viral safety of human blood plasma products. *WHO Technical Report, Series*, 924, 150–224.

Zhang, W., Thompson, K. E., Reed, A. H., & Beenken, L. (2006). Relationship between packing structure and porosity in fixed beds of equilateral cylindrical particles. *Chemical Engineering Science*, *61*(24), 8060–8074. https://doi.org/10.1016/j.ces.2006.09.036

How to cite this article: Hong, M. S., Lu, A. E., Ou, R. W., Wolfrum, J. M., Springs, S. L., Sinskey, A. J., & Braatz, R. D. (2021). Model-based control for column-based continuous viral inactivation of biopharmaceuticals. *Biotechnology Bioengineering*. 118, 3215–3224. https://doi.org/10.1002/bit.27846